



OPEN ACCESS

EDITED BY
Nozomu Takeuchi,
Chiba University, Japan

REVIEWED BY
Shin Sugiyama,
Hokkaido University, Japan
Qiang Liu,
Beijing Normal University, China

*CORRESPONDENCE
Sunil N. Oulkar,
sunil@ncpor.res.in

SPECIALTY SECTION
This article was submitted to
Cryospheric Sciences,
a section of the journal
Frontiers in Earth Science

RECEIVED 21 May 2022
ACCEPTED 01 July 2022
PUBLISHED 12 August 2022

CITATION
Oulkar SN, Thamban M, Sharma P,
Pratap B, Singh AT, Patel LK, Pramanik A
and Ravichandran M (2022), Energy
fluxes, mass balance, and climate
sensitivity of the Sutri Dhaka Glacier in
the western Himalaya.
Front. Earth Sci. 10:949735.
doi: 10.3389/feart.2022.949735

COPYRIGHT
© 2022 Oulkar, Thamban, Sharma,
Pratap, Singh, Patel, Pramanik and
Ravichandran. This is an open-access
article distributed under the terms of the
[Creative Commons Attribution License
\(CC BY\)](https://creativecommons.org/licenses/by/4.0/). The use, distribution or
reproduction in other forums is
permitted, provided the original
author(s) and the copyright owner(s) are
credited and that the original
publication in this journal is cited, in
accordance with accepted academic
practice. No use, distribution or
reproduction is permitted which does
not comply with these terms.

Energy fluxes, mass balance, and climate sensitivity of the Sutri Dhaka Glacier in the western Himalaya

Sunil N. Oulkar^{1,2*}, Meloth Thamban¹, Parmanand Sharma¹,
Bhanu Pratap¹, Ajit T. Singh¹, Lavkush Kumar Patel¹,
Ankit Pramanik¹ and M. Ravichandran^{1,3}

¹National Centre for Polar and Ocean Research, Ministry of Earth Sciences, Goa, India, ²School of Earth, Ocean and Atmosphere Sciences, Goa University, Goa, India, ³Ministry of Earth Sciences, Government of India, New Delhi, India

Various regional climatic factors influence glacier mass balance and thus control the water budget of the Himalayan rivers. However, the scarcity of observational data hinders a detailed understanding of the processes governing glacier mass balances in the Himalaya. Here we analyze the mass balance of the Sutri Dhaka Glacier, a debris-free glacier in the Chandra basin (western Himalaya) combining field observations and a physically based model to understand the drivers of mass balance variability. The modeled energy flux showed that net shortwave radiation contributed 56% to the total surface energy fluxes, followed by net longwave radiation (27%), sensible heat (8%), latent heat (5%), and ground heat flux (4%). However, over the ablation zone, inward fluxes account for most of the total heat flux, resulting in strong summertime melting. The model estimated glacier mass balance was -1.09 ± 0.31 and -0.62 ± 0.19 m w.e. during 2015/16 and 2016/17, which matches well with the *in situ* glaciological mass balance of -1.16 ± 0.33 and -0.67 ± 0.33 m w.e., respectively. A sensitivity analysis demonstrates that the mass balance of the glacier is affected by both air temperature (-0.21 m w.e. $a^{-1} \text{ } ^\circ\text{C}^{-1}$) and precipitation (0.19 m w.e. a^{-1} (10%) $^{-1}$) changes. Our study suggests that, the mass balance of the Sutri Dhaka Glacier is less sensitive to changes in the partitioning of precipitation into snow and rain because the majority of precipitation falls as snow during the winter when the temperature is well below 0°C .

KEYWORDS

energy balance modeling, mass balance, climate sensitivity, Chandra basin, western Himalaya

1 Introduction

The glaciers in the Hindu Kush Himalayan region are the largest reservoir of snow and ice mass outside the polar regions and play a crucial role in supplying meltwater to the major rivers of southwest Asia, which sustain the livelihoods of nearly 1.9 billion people in the downstream region (Dyurgerov and Meier, 2005; Immerzeel et al., 2010; Bolch et al., 2012). Meltwater from the Himalayan glaciers is an important source of water to major rivers, such as Indus, Ganges, and Brahmaputra, especially during the summer months. However, the magnitude of runoff from the Himalayan glaciers is expected to vary in a changing climate, affecting downstream water supply, especially for dry seasons or years (Pritchard, 2019). Among the major basins, the Indus basin in the western Himalaya is the most dependent on snow and glacier melt, with nearly 62% of the total annual discharge contributed by snow and glacier melt, whereas this fraction is significantly less in the Ganges (20%) and Brahmaputra (25%) basins in the central and eastern Himalaya, respectively (Lutz et al., 2014). Thus, glaciers will have a dominant role in the water budget of the Indus River under future climate change scenarios.

Several studies have demonstrated the substantial loss of glacier ice mass, resulting in the rapid retreat of the Himalayan glaciers in the recent decades (Kulkarni et al., 2007; Bolch et al., 2012; Brun et al., 2017; Kumar et al., 2019; Shean et al., 2020). On a regional scale (western, central, and eastern Himalaya), the glaciers have shown enhanced thinning during the past decade except for the Karakoram and adjacent regions (Kääb et al., 2012; Gardelle et al., 2013; Farinotti et al., 2020). However, due to the remoteness and high-altitude terrain of Himalayan glaciers, *in situ* hydrometeorological measurements are limited to very few glaciers (Pratap et al., 2016; Azam et al., 2018; Kumar et al., 2018; Azam et al., 2019; WGMS, 2019). Thus, the relationship between atmospheric forcing and glacier mass change in the Himalaya is poorly understood. Therefore, it is essential to understand the response of glaciers to atmospheric forcing using hydrometeorological observations and numerical models. Although an empirical temperature index model (Hock, 2003) is convenient for modeling glacier mass balance using air temperature (T_{air}) and precipitation, this simple model does not track the energy fluxes. The energy balance model approach, which considers different energy fluxes interacting with glaciers, is considered to be very effective for simulating the distributed mass balance of glaciers and are also valuable for detailed sensitivity studies of glacier mass balance (Oerlemans and Reichert, 2000; De Woul and Hock, 2005; Li et al., 2019).

Within the Himalaya, the Western Disturbance (WD) and the Indian Summer Monsoon (ISM) are the dominant sources of precipitation and significantly affect the mass balance of the

glaciers (Shekhar et al., 2010; Azam et al., 2014a). While WD plays a dominant role in determining glacier behavior in the western Himalaya, the ISM plays more important role in the central and eastern Himalaya. The WDs mainly contributes to the winter precipitation events in the upper Indus Basin, which are driven by the approaching extra-tropical, synoptic-scale disturbances (Dimri et al., 2015; Jean-Philippe et al., 2021). One of the major sub-basins of the upper Indus basin is the Chandra basin, which lies in the transition zone of WD and ISM (Bookhagen and Burbank, 2006). Since the Chandra River is passing through a semi-arid zone, its water budget is highly sensitive to the melting of snow and glaciers. With the recent increases in extreme events of precipitation and increasing temperature, the Chandra basin provides an ideal testbed to understand the status and climate sensitivity of glaciers from western Himalaya.

To understand the spatio-temporal variability in surface energy and mass balance, it is important to undertake integrated studies using *in situ* measurements and by employing energy balance models that can simulate the distributed mass balance. Towards this, we examine the Sutri Dhaka Glacier from the upper Chandra basin, a relatively large (~20 km²) and debris-free glacier, during two contrasting meteorological years using field data and a well-constrained physically based COupled SNOWpack and Ice surface energy and MAss balance model (COSIMA) (Huintjes et al., 2015). The model is forced with meteorological data obtained from an on-glacier Automatic Weather Station (AWS). We calibrate the model with meteorological and glaciological data from point locations and then use the model to simulate the mass balance for the entire glacier. This study allows us to assess the mass balance sensitivity of the Sutri Dhaka Glacier to different atmospheric variables and investigate the importance of snow-to-rain conversion during warmer years in amplifying the temperature sensitivity of the mass balance.

2 Study area

The Chandra basin has 201 glaciers, covering an area of 703.6 km², having large differences in size, surface characteristics, and orientation/aspect (Sangewar and Shukla, 2009). Many glaciers of the upper Chandra basin have different aspect/orientation and may experience differences in the energy budget, especially the net shortwave radiation (Patel et al., 2021). The Sutri Dhaka Glacier is the third largest glacier of the upper Chandra basin (Figure 1). It covers an area of ~20 km², with a length of ~10.7 km along a north-east orientation. It is a debris-free glacier with only 5% of the ablation area covered with thin debris (Sharma et al., 2016). The glacier elevation ranges from 4,500 m a.s.l. at the snout to 6,000 m a.s.l. at the bergschrunds with an average slope of ~10° (Pratap et al.,

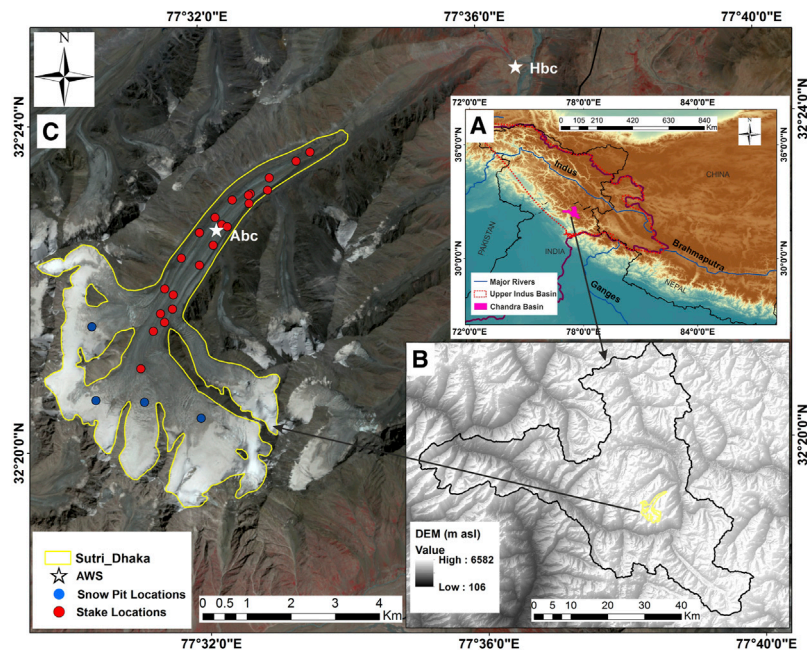


FIGURE 1
 Location map (A) of the study region in the western Himalaya, (B) the Chandra basin, and (C) the Sutri Dhaka Glacier (yellow outline) with the location of two AWS (white stars) located at Abc (4,864 m a.s.l.) and Hbc (4,052 m a.s.l.). The red dots represent the ablation stakes installed, and the blue dots are accumulation pit locations.

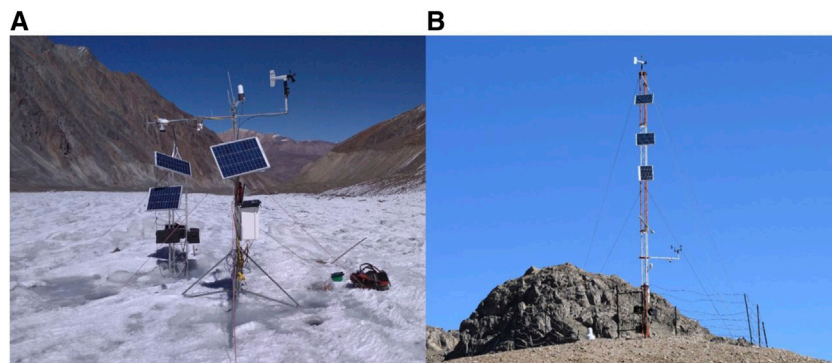


FIGURE 2
 Field photos of the AWSs (A) fixed on the glacier surface at Abc (4,864 m a.s.l.) and (B) installed on the open ground at Hbc (4,052 m a.s.l.). Locations of these AWSs are marked in Figure 1.

2019). This glacier is a part of the long-term monitoring project by the National Centre for Polar and Ocean Research (NCPOR) since 2013, and meteorological observations started in 2015.

The study region lies in the ISM-WD transition zone and the climate is dominated by relatively long winters (November–March). The glacier is located in the northern limit of the ISM and also experiences a leeward effect,

therefore less amount of annual precipitation occurs during the ISM (June–September), while a significant amount of precipitation occurs in the form of snowfall during the winter as a result of active WDs (Singh et al., 2019). Furthermore, the balance year on the Sutri Dhaka Glacier is defined as 1st October to 30th September, following the approach at nearby Chhota Shigri Glacier (Wagnon et al., 2007).

TABLE 1 List of hydrometeorological variables measured at the AWSs used in the study.

Variables	Sensor type	Measurement range	Accuracy	Measurement height (m) Abc (Hbc)
Air Temperature	Campbell HC2S3	-50°C to +60°C	±0.1°C	2 (2.2)
Relative Humidity	Campbell HC2S3	0–100% RH	±0.8% RH	2 (2.2)
Wind Speed & Wind Direction	RM Young Sensor 05103	0–100 m s ⁻¹	±0.3 m s ⁻¹ & ±3° Direction	3.8 (3.4)
Surface Temperature	Campbell SI-111	-55 to 80°C	±0.5°C at -40 to 70°C	3.6 (4.2)
Solar Radiation (Incoming & Outgoing)	Kipp & Zonen CNR4	0 to 2000 Wm ⁻²	±10%-day total	3.6 (4.2)
Longwave Radiation (Incoming & Outgoing)	Kipp & Zonen CNR4		±10%-day total	3.6 (4.2)
Precipitation	OTT Pluvio ²	12–1800 mm/h	±0.05 mm	- (0)

TABLE 2 The mean annual altitudinal gradient/lapse rates calculated from Abc, Hbc and ERA5 for extrapolation of data.

Variables	Altitudinal gradient
Elevation (m a.s.l.)	4,500–6,000
Air temperature lapse rate (°C m ⁻¹)	-0.0042
Precipitation gradient (% m ⁻¹)	0.12
Air pressure gradient (hPa m ⁻¹)	-0.034
Relative humidity lapse rate (% m ⁻¹)	0.012

3 Data collection and methodology

3.1 Field measurements and data processing

3.1.1 Meteorological data

Two AWS systems (Campbell Scientific) have been operating at the Sutri Dhaka Glacier catchment since October 2015 (Figure 1C). One AWS is situated on the glacier surface in the upper ablation zone at Advance base camp (Abc, 4,864 m a.s.l.), while the other is located on the open ground in the same catchment at the HIMANSH base camp (Hbc, 4,052 m a.s.l.) (Figure 1C, Figures 2A,B). The distance between Abc and Hbc is 8 km, with an altitudinal difference of 812 m. The details of the AWS sensors are listed in Table 1 including their accuracy and measurement range. The data are stored by the dataloggers at every 10-min interval.

There was a data gap during the 2017 summer, as the AWS at Abc stopped functioning from 25th to 30th June owing to a power cut. The data gap in T_{air} and relative humidity at Abc were filled with linearly extrapolated data from the station Hbc using a lapse rate (Table 2 and Figure 3). Additionally, hourly net shortwave (S_{net}) radiation, net longwave (L_{net}) radiation, wind speed, and albedo data were obtained from the European Centre for Medium-Range Weather Forecasts (ECMWF) reanalysis (ERA5) at the nearest surface grid points of Abc and used to fill the data gap using bias correction. Due to the malfunctioning

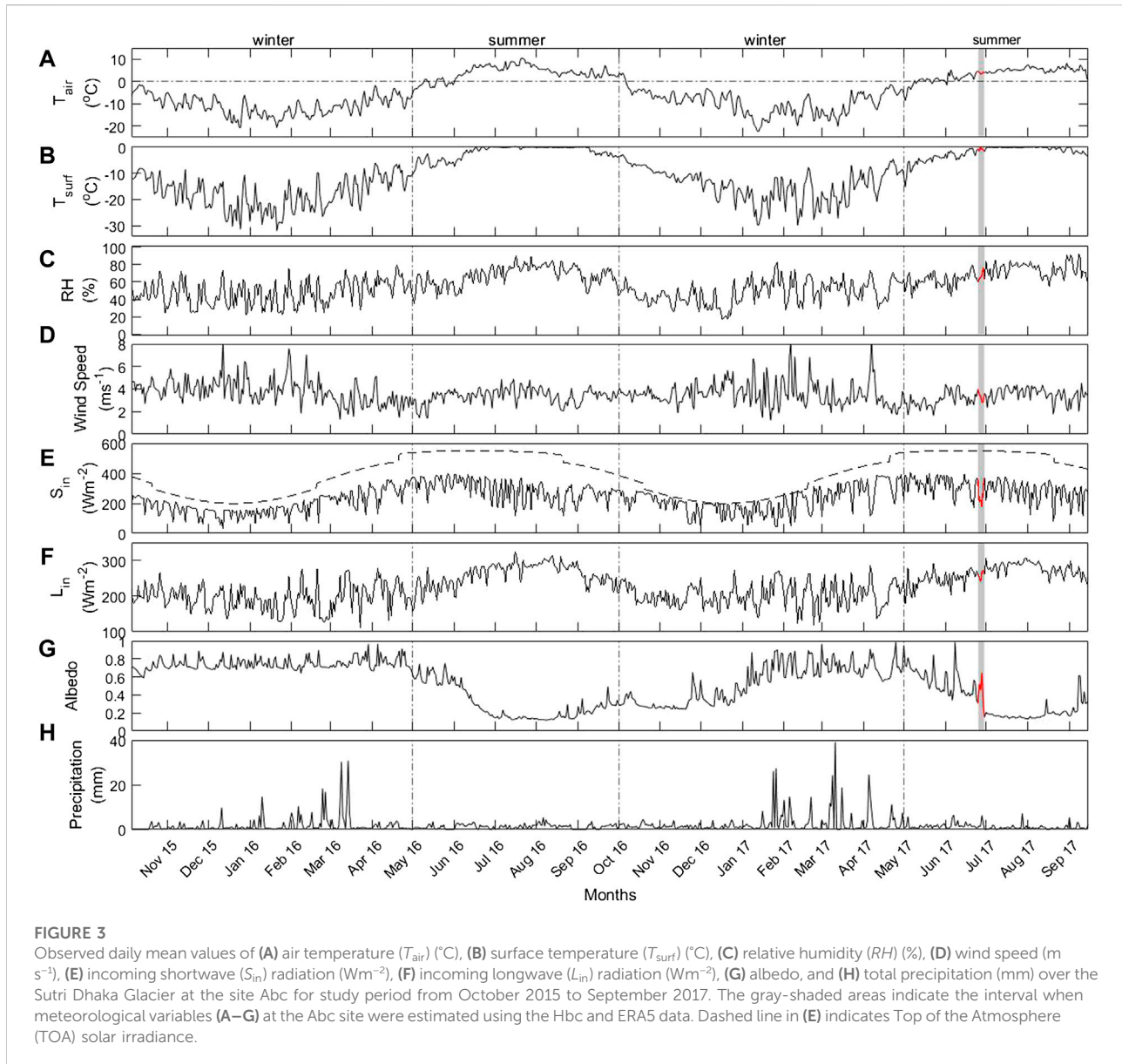
of the precipitation sensor at Abc, only Hbc precipitation data were used for analysis. Furthermore, air pressure data at an hourly resolution were obtained from the ERA5 for the nearest surface level at the two-point location of Abc. It was corrected from the ERA5 pixel elevation to the on-glacier site Abc using the air pressure lapse rate. Cloud cover for the study region was estimated based on L_{net} and T_{air} following the procedure by Van Den Broeke et al. (2006), which calculates a quantitative cloud cover fraction estimate ranging between 0 and 1.

The mean annual lapse rates were calculated with the observed meteorological data obtained from Abc, Hbc, and ERA5 data (Table 2). The monthly T_{air} lapse rate of the catchment ranges from -0.0003 to -0.0065°C m⁻¹, with a mean of -0.0042°C m⁻¹. The monthly relative humidity lapse rate varied from 0.009 to 0.016% m⁻¹ (mean 0.012% m⁻¹). The monthly air pressure gradient calculated from grid points of ERA5 data nearest to the two AWS, ranged from -0.026 to -0.049 hPa m⁻¹ (mean -0.034 hPa m⁻¹). For the observation period from 4th October 2015 to 15th September 2017, at all stake points, we calibrate the estimated mass balance using various precipitation gradient values and use the lowest root mean square error (RMSE) between modeled and measured mass balance. The precipitation gradient is derived from the model calibration process. The precipitation gradient value used in the study is 0.12% m⁻¹ (Supplementary Figure S1).

A digital elevation model (DEM) with a spatial resolution of 30 m obtained from the ASTER GDEM V2 from Earth Remote Sensing Data Analysis Centre (ERSDAC) (Tachikawa, 2011) was resampled bilinearly to a 45 m grid resolution. Based on the gradient (precipitation and air pressure) and lapse rate (T_{air} and relative humidity), we extrapolated the meteorological data at the grid points of the resampled 45 m DEM to obtain distributed surface energy and mass balance of the Sutri Dhaka Glacier (Table 2).

3.1.2 Glaciological surface mass balance and uncertainty

The surface mass balance of the Sutri Dhaka Glacier was measured using the *in situ* glaciological method following established methodologies (Østrem and Brugman, 1991;



Cogley et al., 2011). The annual ablation and accumulation measurements were performed at the end of the ablation season (i.e., end of September). Ablation was measured using a network of stakes, and accumulation was measured through excavating snow pits or snow coring (Kovacs Mark II) at various locations on the glacier (Figure 1C). A network of 30–35 ablation stakes was drilled into the ice over the glacier surface along with different altitudinal zones for both study years (Figure 1C). These stakes were measured throughout the summer season for ablation estimation using exposed stake heights. Ice density for the ablation zone was considered to be $870\ kg\ m^{-3}$ ($\pm 25\ kg\ m^{-3}$, $n = 10$), and the snow density of $490\ kg\ m^{-3}$ ($\pm 30\ kg\ m^{-3}$, $n = 8$), which was measured in the field at the end of ablation season (Pratap et al., 2019). The accumulation zone of the glacier for

glaciological measurement was accessible up to $\sim 5,700\ m\ a.s.l.$ To estimate the total accumulation, snow density, snow water equivalent, and depth measurements were extrapolated for the entire accumulation area. Mass balance was calculated using the sum of accumulation and ablation, and integrated over the entire glacier surface area. The glacier-wide average annual mass balance is calculated using:

$$B = \frac{1}{S} \sum b_n s_n \quad (1)$$

where B is glacier-wide average annual mass balance, b_n is the mass balance of the altitudinal range, s_n is the area of corresponding ablation or accumulation altitudinal range, and S is the total area of the glacier.

The potential annual mass balance uncertainties in the *in situ* observations are related to: 1) the uncertainties in ablation estimates related to stake height measurements and ice density; 2) the uncertainties in accumulation observations of snow depth and snow density; and 3) the uncertainty related to the extrapolation of point measurements of corresponding altitudinal bands and the entire glacier (Thibert et al., 2008). The uncertainties in stake height measurements could be due to the mean height difference. Although we chose a representative surface in its vicinity to install the stakes, the variability associated with the surface morphological changes (e.g., meltwater channels, boulders, and avalanches) cannot be evaluated. Rather we exclude those stakes with such uncertainties from the final calculation. Therefore, the propagated uncertainty associated with extrapolation of the ablation was ± 0.19 m w.e. a^{-1} . Furthermore, we calculated the uncertainty in accumulation measurements following the approach by Kenzhebaev et al. (2017): 1) the uncertainties in snow density were estimated as ± 30 kg m^{-3} for calculation of the accumulation; 2) we used 0.22 m w.e. $(100\text{ m})^{-1}$ as the accumulation gradient measured at the Chhota Shigri Glacier (Azam et al., 2016) to approximate a linear increase in accumulation; and 3) for the two uppermost altitude bins, an inverse gradient is adopted. The uncertainty in accumulation measurements (± 0.28 m w.e. a^{-1}) was calculated using the mean of standard deviations obtained using the methods described above. Taking all of the errors into account, an overall uncertainty in observed mass balance at the Sutri Dhaka Glacier was calculated as ± 0.33 m w.e. a^{-1} . This is well within the estimated uncertainties of the glaciological methods ranging from ± 0.27 to ± 0.53 m w.e. for various Himalayan glaciers (Azam et al., 2012; Wagnon et al., 2013; Sunako et al., 2019; Mandal et al., 2020; Soheb et al., 2020).

3.2 Model

3.2.1 Surface energy balance model

To simulate the distributed surface energy and mass balance, we used the COSIMA model, which is an open source physically based energy balance model for high mountain glaciers. COSIMA 1D model is a point energy and mass balance model for one-dimensional use at a single location. Meanwhile, COSIMA 2D model is a two-dimensional model for spatially distributed surface energy and mass balance studies. The parameterization of subsurface energy and mass fluxes within COSIMA is directly coupled to the surface processes, as in other widely used surface energy and mass balance studies (Klok and Oerlemans, 2002; Hock and Holmgren, 2005; Pellicciotti et al., 2009). The COSIMA model includes several modules that solve the heat equation and calculate surface temperature and energy balance, meltwater percolation, refreezing, and densification (Huintjes et al., 2015). It

explicitly calculates the percolation of meltwater and the refreezing process within the snowpack, taking into account the latent heat flux release and resulting subsurface melt, as well as the effects on subsurface temperature, snow density, and the ground heat flux. Furthermore, COSIMA can effectively estimate the mass balance by explicitly calculating the effects of radiation, aging, and albedo changes on the snow surface, vertical heat transport in the snow, densification of snow with depth, and liquid water retention (Huintjes et al., 2015). In addition to the full energy balance on the surface, adding snowpack to the multi-layer vertical dimension of the model enables an explicit simulation of vertical heat diffusion, percolation of liquid water from melting and rain, the refreezing of liquid water and internal accumulation, and a realistic representation of firn densification due to overloading and refreezing (Huintjes et al., 2015; Singh et al., 2018).

The model is forced by meteorological data, including T_{air} , relative humidity, total precipitation, wind speed, air pressure, incoming shortwave radiation, and cloud cover fraction. In this study, hourly data of meteorological variables along with the resampled 45 m DEM were used to derive the spatial distribution of surface energy and mass balance of the Sutri Dhaka Glacier. The total energy flux at the glacier surface is calculated within the COSIMA model (Oerlemans, 2001; Huintjes et al., 2015), as follows:

$$Q = S_{\text{in}}(1 - \alpha) + L_{\text{in}} + L_{\text{out}} + H_{\text{se}} + H_{\text{la}} + Q_{\text{G}} \quad (2)$$

where Q is the total heat flux, S_{in} is incoming shortwave radiation, α is the surface albedo, L_{in} is incoming longwave radiation, L_{out} is outgoing longwave radiation, H_{se} is turbulent sensible heat flux, H_{la} is turbulent latent heat flux, and Q_{G} is ground heat flux. Heat flux from liquid precipitation is negligible and hence neglected in the model (Huintjes et al., 2015). All energy fluxes are expressed in Wm^{-2} , and are defined as positive when it is towards the surface of the glacier and negative when away from the surface. The resulting flux Q leads to surface melt energy (Q_{melt}) only when the surface temperature is at the melting point (0°C).

We separately calculated the S_{in} , following the approach by Huintjes et al. (2015). First, a solar radiation model by Kumar et al. (1997) was used to compute clear-sky and diffuse incoming shortwave radiation (S_{pot}) without considering the cloud effect at Abc with no shading. The cloud effect of the S_{pot} was corrected with incoming shortwave radiation data of Abc to determine the correction factor, which is further used in the study to spatially derive S_{in} . The modeled L_{in} and L_{out} were estimated using the Stefan-Boltzmann law (Klok and Oerlemans, 2002). The turbulent heat fluxes H_{se} and H_{la} are calculated using the bulk aerodynamic method with correction of stability (Oerlemans, 2001). The bulk transfer coefficients for H_{se} and H_{la} depend on instrument height (z), and surface roughness length (z_0). The z_0 changes depending on time from fresh to aged snow (Mölg and Scherer, 2012). The z_0 increases linearly from

0.24 mm for fresh snow (Gromke et al., 2011) to 4 mm for aged snow (Brock et al., 2006), whereas z_0 is assumed to be 1.7 mm for the snow-free surface (Cullen et al., 2007). The Q_G consists of fluxes due to heat conduction and penetrating shortwave radiation (Q_{ps}). The Q_{ps} remains negative because it only transfers energy from the glacier surface into the snow or ice. At each DEM pixel, the glacier surface characteristics are controlled by surface temperature and albedo, which were determined in COSIMA at each time step and changed linearly over time from fresh to aged snow.

The parameterization of surface albedo (α) follows the scheme of Oerlemans and Knap (1998), where α is determined as a function of snowfall frequency and snow depth:

$$\alpha_{\text{snow}} = \alpha_{\text{firn}} + (\alpha_{\text{firsnow}} - \alpha_{\text{firn}}) \exp(t_{\text{snow}} t^*{}^{-1}) \quad (3)$$

$$\alpha = \alpha_{\text{snow}} + (\alpha_{\text{ice}} - \alpha_{\text{snow}}) \exp(-h d^*{}^{-1}) \quad (4)$$

The free parameters of the surface albedo scheme are determined according to Mölg and Scherer (2012) and measurements at Abc between 2015 and 2017. The values are: fresh snow albedo (α_{firsnow}) = 0.9, firn albedo (α_{firn}) = 0.55, and ice albedo (α_{ice}) = 0.2. However, t_{snow} is the time since the last snowfall, t^* is constant (6 days) for the effect of aging on snow albedo, h is the snow depth, and d^* is a constant (8 cm) for the effect of snow depth on albedo.

The COSIMA subsurface model uses a vertical layer structure that consists of layers with an equal thickness of 0.2 m. The temperature, density, and depth are characterized by each subsurface ice layer. The initial temperature profile was interpolated linearly between T_{air} and surface temperature. In each time step, the surface temperature profile is calculated from the thermodynamic heat equation (Huintjes et al., 2015). Initial snow depth is set to zero with the start of the balance year (i.e., 1st October). Thus, the subsurface density profile is initialized with a constant glacier ice density of 870 kg m⁻³ and a snow density of 490 kg m⁻³ based on field observations (Pratap et al., 2019). The values for site-specific constants within the COSIMA model are adopted from Klok and Oerlemans (2002) and Huintjes et al. (2015) for simulations at the Sutri Dhaka Glacier.

3.2.2 Sensitivity experiments

To assess climate sensitivity in this study, we perturbed the meteorological variables according to climatic factors and associated simulations (Yang et al., 2011; Yang et al., 2013; Sun et al., 2018; Zhu et al., 2018; Li et al., 2019). We performed sensitivity experiments for mass balance by changing the assumed value for one input parameter at a time, leaving all other parameters unchanged. The ranges of the perturbation were $\pm 1^\circ\text{C}$ for T_{air} , $\pm 10\%$ for relative humidity, $\pm 50 \text{ W m}^{-2}$ for S_{in} , $\pm 10\%$ for total precipitation, and $\pm 1 \text{ m s}^{-1}$ for wind speed throughout the period.

3.2.3 Model uncertainty assessment using Monte Carlo simulations

Estimating uncertainty in complex models based on analytical solutions is extremely difficult when the set of uncertain variables is large and nonlinear effects exist. Therefore, the model uncertainty was estimated using the Monte Carlo simulations (Van Der Veen, 2002). The model uncertainty was estimated based on repeated modeling of the mass balance at all observed point locations on the Sutri Dhaka Glacier. A model run was repeated 100 times in the Monte Carlo simulation, in which the normally distributed model parameters and threshold were varied by 10% and the input variables were randomly varied within their uncertainty ranges to estimate the final uncertainty (Machguth et al., 2008). The mass balance uncertainty of 100 simulations was evaluated using standard deviation. We found that the difference between the observed and the modeled mass balance is within the range of uncertainty of 100 simulations (Supplementary Figure S2). The overall uncertainty of modeled mass balance was $\pm 25\%$.

4 Results

4.1 Meteorological conditions at the Sutri Dhaka catchment

The meteorological data for the two balance years (2015/16 and 2016/17) obtained from the on-glacier site Abc are shown in Figure 3. Over the study period, daily T_{air} varied from 10.0 to -22.4°C (Figure 3A). The mean values were -4.6 and -4.4°C for the balance years 2015/16 and 2016/17, respectively. However, the daily surface temperature varied from 0 to -31.9°C with the mean values of -11.0 (2015/16) and -9.6°C (2016/17) (Figure 3B). The daily mean T_{air} was above 0°C between early June and the end of September. The data shows that January was the coldest month and August was the warmest month in this glacierized basin, in agreement with other studies on nearby glaciers (Azam et al., 2014a). During the summer, surface temperature remains close to the melting point in agreement with consistently positive T_{air} (Figures 3A,B). Daily relative humidity varied from 4 to 92%, with mean values of 56% ($\pm 16\%$) (Figure 3C). The area was characterized by a warm summer with high relative humidity from June to September and a cold winter season, which is comparatively less humid, from December to February. The daily mean wind speed varied between 1.2 and 8.5 m s⁻¹ with a mean speed of 3.6 m s⁻¹ ($\pm 1 \text{ m s}^{-1}$) (Figure 3D). The observed wind direction during the study period was mostly downslope, with a maximum speed of 13.5 m s⁻¹, suggesting predominately katabatic flow with modest strength over the glacier. The winter period was characterized by high wind speed with larger variability ($\pm 1.2 \text{ m s}^{-1}$), whereas the wind speed in the summer was comparatively less varied

($\pm 0.5 \text{ m s}^{-1}$) (Figure 3D). The mean daily values of S_{in} varied from 84 to 403 Wm^{-2} in summer and 30 to 385 Wm^{-2} in winter for both the balance years (Figure 3E). The annual mean was 248 and 223 Wm^{-2} for the balance years 2015/16 and 2016/17, respectively (Figure 3E). Summers are characterized with intense solar heating, whereas winters are associated with cold, dry, and windy conditions due to low Sun elevation and strong westerlies. The variation of L_{in} in the summer was 178–324 Wm^{-2} , and in the winter, it was 112–306 Wm^{-2} for both the balance years (Figure 3F). The annual mean was 223 Wm^{-2} and 227 Wm^{-2} for the balance year 2015/16 and 2016/17, respectively (Figure 3F). During the summer, higher L_{in} can be associated with cloudy days, whereas during the winter its variability is higher, which can be due to significant fluctuation in cloud conditions. At the on-glacier site Abc, albedo ranges between 0.20 and 0.98, with a mean value of 0.35 (2015/16) and 0.41 (2016/17) (Figure 3G). The Abc location exhibited a higher mean albedo in winter (0.74) than in summer (0.31), due to the contrasting surface conditions of fresh snow versus glacier ice, respectively. The annual precipitation was 567 and 710 mm for the balance years 2015/16 and 2016/17, respectively. In both the balance years (2015/16, 2016/17), higher precipitation occurred during the winter (60%, 80%, respectively) than the summer (40%, 20%, respectively) (Figure 3H).

4.2 Model calibration

The COSIMA 1D model was used to assess the efficiency at several sites where calculations were done for one grid point, providing a quick and efficient technique to test the model performance. Initially, a set of observed hourly meteorological data were used as input data to run the COSIMA 1D model at the Abc site (Figure 1C) for the period from 4th October 2015 to 15th September 2017. Furthermore, the 1D model results were evaluated against the observed surface temperature, L_{net} , and albedo. Within the model, the initial temperature profile was simulated linearly between air and surface temperature; correspondingly, the surface roughness is determined based on fresh snow, aged snow, and ice (Mölg and Scherer, 2012). The approach of Oerlemans and Knap (1998) is used for the parameterization and initial conditions of the surface albedo, as shown in Eq. 4. These estimated variables (surface temperature, L_{net} , and albedo) obtained from the 1D model were compared with the observed Abc data. We found a strong correlation between the modeled and observed Abc data for surface temperature ($r = 0.96$; $n = 712$, mean absolute error=1.15°C), L_{net} ($r = 0.92$; $n = 712$, mean absolute error=20.59 Wm^{-2}), and albedo ($r = 0.89$; $n = 712$, mean absolute error=0.09) for the period from 4th October 2015 to 15th September 2017 (Figure 4).

The observed mass balance for the nearest ablation stake ($\sim 5 \text{ m}$ from Abc site, 4,863 m a.s.l.) was -4.30 ± 0.33 and $-3.59 \pm 0.33 \text{ m w.e.}$ and the calibrated modeled surface mass balance at

Abc site was -3.98 ± 0.99 and $-3.34 \pm 0.84 \text{ m w.e.}$ for the balance year 2015/16 and 2016/17, respectively. Furthermore, we plotted the observed annual balances (point-wise) with the modeled annual balance at the corresponding grid location (Figure 5). The coefficient of determination (R^2) between the simulation and the measurement for the surface mass balance was 0.97 (RMSE=0.38 m w.e.) for 2015/16 and 0.98 (RMSE=0.58 m w.e.) for 2016/17, respectively (Figure 5). The modeled (observed) annual mass balance gradient between 4,500 and 5,500 m a.s.l. was 0.8 (0.87) m w.e. (100 m) $^{-1}$ and 0.79 (0.9) m w.e. (100 m) $^{-1}$ for the balance year 2015/16 and 2016/17, respectively. Overall, the model has an excellent ability to simulate the mass balance processes of the Sutri Dhaka Glacier and performed well for the study period from 4th October 2015 to 15th September 2017.

4.3 Surface energy balance

4.3.1 Distributed surface energy balance

The simulated spatial variability of S_{net} and L_{net} , the turbulent heat fluxes (H_{se} and H_{la}), albedo and Q_G averaged over two balance years (2015/16 and 2016/17) are shown in Figure 6. The results obtained by the COSIMA 2D model show that mean S_{net} ranges from 20 to 200 Wm^{-2} (Figure 6A) and varies with altitude, where the S_{net} decreases as the mean albedo increases (Figures 6A,B). The mean L_{net} flux varied from -120 to -70 Wm^{-2} and decreased with the altitude (Figure 6C). The turbulent heat fluxes of H_{se} and H_{la} both showed maximum values over the lower ablation zone (Figures 6D,E). High values at the lower parts and decreasing values with increasing altitude can be explained by the temperature gradient against elevation. The modeled longwave radiation and turbulent heat fluxes depend mainly on T_{air} and relative humidity as a function of altitude (Klok and Oerlemans, 2002; Mölg et al., 2009). Simulated Q_G heat flux is mainly a function of surface temperature and topographic characteristics; therefore, it is lowest in the accumulation area (Figure 6F), where the surface temperature is minimum.

4.3.2 Seasonal and annual contribution of energy fluxes

We demarcated the accumulation and ablation area of the glacier based on the observed mean equilibrium line altitude (ELA) (5,300 m a.s.l.). The contribution of the energy fluxes was separately estimated for accumulation, ablation, and glacier-wide zone based on the simulation (Figure 7: Supplementary Figure S3). In the accumulation and ablation zones, surface energy exchanges happen due to distinct climatic characteristics (Wu et al., 2016).

In the accumulation zone, the mean energy fluxes during the winter (2015/16 and 2016/17) were predominantly governed by outward L_{net} (Figure 7). The outward flux contribution was higher than the inward flux, which suggested that the cooling

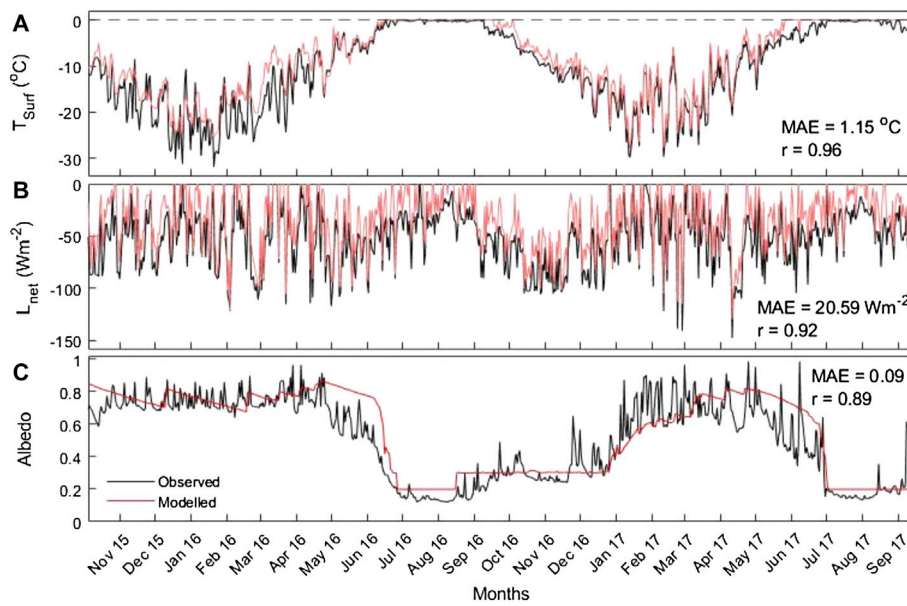


FIGURE 4
 Observed (black) and modeled (red) daily mean values of (A) surface temperature (T_{surf}) ($^{\circ}C$), (B) net longwave (L_{net}) radiation (Wm^{-2}), and (C) albedo with their correlation coefficient at the Abc site for the Sutri Dhaka Glacier from October 2015 to September 2017.

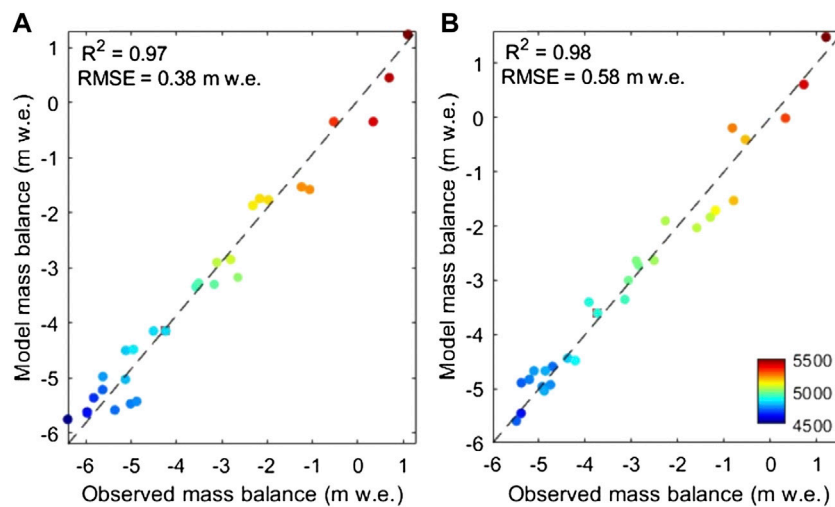


FIGURE 5
 Comparison of observed and modeled mass balance (m w.e.) at the Sutri Dhaka Glacier for two contrasting meteorological years: (A) 2015/16 and (B) 2016/17.

effect was dominant. However, it was primarily contributed by inward S_{net} and outward L_{net} during the summer (Figure 7). The total energy increased the temperature of the snowpack; however, the available energy only marginally exceeded the cold content of the snowpack. Throughout the study period, in the accumulation

zone, higher contributions of outward H_{la} and Q_G heat flux suggests that there was maximum cooling effect. In the ablation zone of the glacier, during the winter (2015/16 and 2016/17), the mean energy fluxes were primarily contributed by inward S_{net} and outward L_{net} , whereas the summers showed dominant

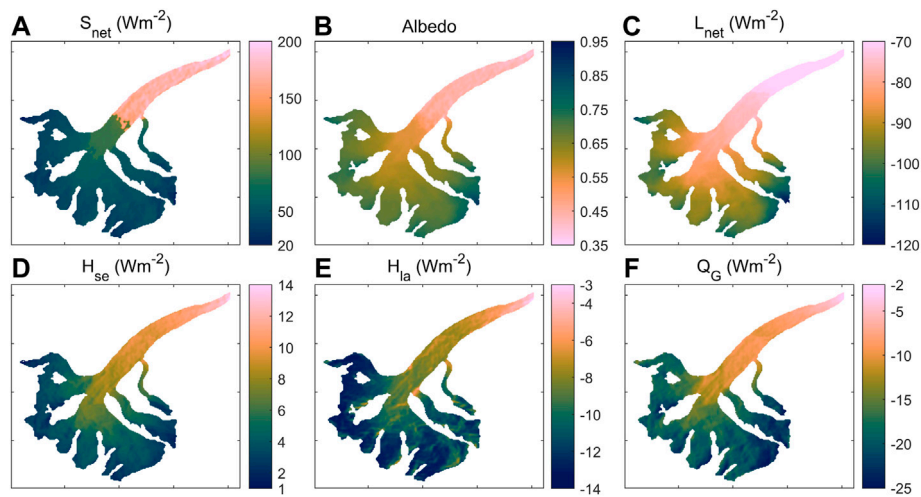


FIGURE 6 Spatial distribution of modeled mean surface energy fluxes for the Sutri Dhaka Glacier over two balance years 2015/16 to 2016/17. **(A)** Net shortwave (S_{net}) radiation, **(B)** albedo, **(C)** net longwave (L_{net}) radiation, **(D)** sensible heat flux (H_{se}), **(E)** latent heat flux (H_{la}), and **(F)** ground heat flux (Q_G).

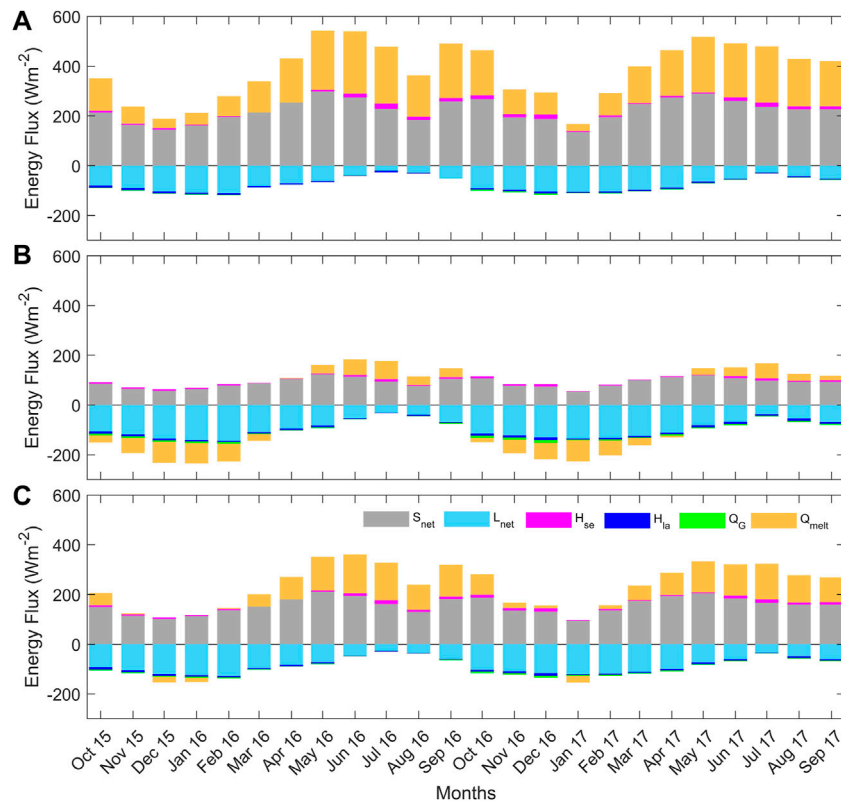


FIGURE 7 The monthly mean surface energy fluxes for the **(A)** ablation zone (below 5,300 m a.s.l.), **(B)** accumulation zone (above 5,300 m a.s.l.), and **(C)** glacier-wide region of the Sutri Dhaka Glacier.

TABLE 3 Comparison of the characteristics and mean annual surface energy fluxes (Wm^{-2}) for various Himalayan glaciers. Values in square brackets are the % contribution of each energy fluxes.

Glacier	Sutri Dhaka	Chandra basin glaciers	Pindari	Chhota Shigri	Zhadang
Region	Western Himalaya	Western Himalaya	Central Himalaya	Western Himalaya	Central Tibetan Plateau
Period of observation	October 2015 to September 2017	October 2013 to September 2019	June 2016 to July 2017	July 2013 to October 2013	October 2009 to September 2011
Altitude (m a.s.l.)	4,500–6,000	4,000 to 6,200	3,750	4,670	5,660
Latitude	32.38°N	30.08 to 32.45°N	30.26°N	32.28°N	30.47°N
S_{net}	157 [56]	64 [59]	[62]	–	69 [45]
L_{net}	–85 [27]	–88 [16]	[24]	–	–52 [37]
$R_{\text{net}} = S_{\text{net}} + L_{\text{net}}$	72 [83]	85 [75]	[86]	87 [80]	17 [82]
H_{se}	7 [8]	15 [15]	[12]	31 [13]	14 [10]
H_{la}	–5 [5]	–11 [8]	[2]	11 [5]	–9 [6]
Q_{G}	–3 [4]	–2 [2]	–	4 [2]	–1 [2]
References	Present study	Patel et al. (2021)	Singh et al. (2018)	Azam et al. (2014b)	Zhang et al. (2013)

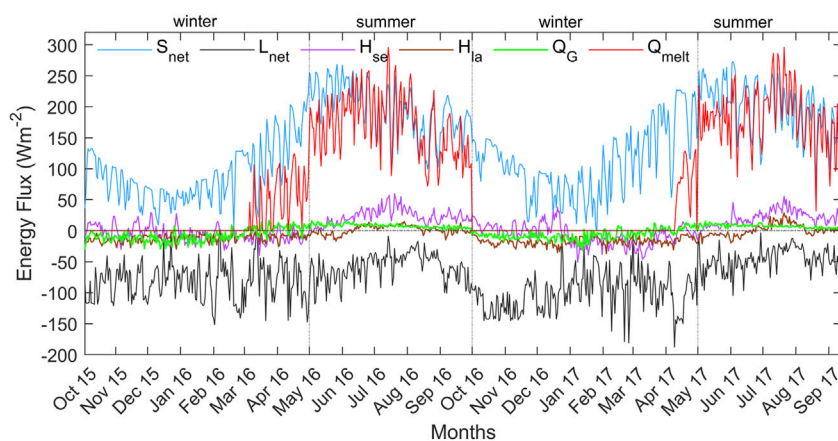


FIGURE 8

Modeled daily mean values of surface energy fluxes at the Sutri Dhaka Glacier from October 2015 to September 2017. S_{net} is net shortwave radiation, L_{net} is net longwave radiation, H_{se} is sensible heat flux, H_{la} is latent heat flux, Q_{G} is ground heat flux, and Q_{melt} is the available melt energy flux.

contribution by inward S_{net} (Figure 7). The S_{net} , accounted for 77% of the total heat flux during the summer, resulting in strong summertime melting in the ablation zone of the Sutri Dhaka Glacier.

The glacier-wide mean annual energy flux showed that S_{net} accounted for 56% of the total surface energy fluxes, followed by L_{net} (27%), H_{se} (8%), H_{la} (5%), and Q_{G} (4%) (Supplementary Figure S3 and Table 3). The winter budget of S_{net} was mainly determined by albedo, which remains very high as the glacier surface is covered by snow (winter time mean albedo ~ 0.74), and this leads to low S_{net} (Figures 3G, Figures 8). Therefore, the available surface energy (Q_{melt}) was significantly less during the

winter and this part of the energy source (S_{net}) was compensated collectively by the energy sink of L_{net} , the turbulent heat fluxes ($H_{\text{se}} + H_{\text{la}}$), and Q_{G} . During the summer, S_{net} was the largest source of energy to the glacier surface and mainly controlled the temporal variability of surface melt, as a result, Q_{melt} followed the same oscillation trend as S_{net} (Figure 8). The contribution of S_{net} (L_{net}) was slightly high (less); that is, 7% more in the 2015/16 balance year than in 2016/17. As a result, summertime melting is more intense, with Q_{melt} contributing more in 2015/16 than in 2016/17 (Table 4). During the summer, clear-sky days with high air and surface temperature gradients were advantageous for H_{se} to heat the glacial surface, resulting in strong summertime

TABLE 4 The modeled seasonal and annual mass balance (m w.e.), as well as the observed annual mass balance (m w.e.), modeled (observed) equilibrium line altitude (ELA; m a.s.l.), and accumulation area ratio (AAR) of the Sutri Dhaka Glacier.

Year	Modeled winter	Modeled summer	Modeled annual	Observed annual	Modeled ELA	Observed ELA	Modeled (Observed) AAR
2015/16	1.99 ± 0.48	-3.07 ± 0.77	-1.09 ± 0.31	-1.16 ± 0.33	5,368 ± 10	5,398 ± 55	0.52 (0.48)
2016/17	2.08 ± 0.52	-2.72 ± 0.69	-0.62 ± 0.19	-0.67 ± 0.33	5,291 ± 12	5,295 ± 69	0.59 (0.58)

melting of the Sutri Dhaka Glacier (Figure 8). The negative H_{la} values (Figure 8) suggest that the only mass loss during the winter was in the form of sublimation. The estimated mass loss due to sublimation, results in a daily mean rate of 0.0013 m w.e. d^{-1} . However, during the summer, H_{la} was positive due to high T_{air} and relative humidity associated with the summer-monsoon circulation, giving rise to deposition at the glacier surface (Figures 3A,C, Figure 8). Such phenomena have also been reported at the Chhota Shigri Glacier (western Himalaya) and AX010 Glacier (central Himalaya) (Kayastha et al., 1999; Azam et al., 2014b). The energy released from condensation leads to positive H_{la} increasing surface melting during the summer (Oerlemans, 2000; Giesen et al., 2009). A negative value for Q_G suggests an increase of the subsurface cold content during the winter, whereas a positive Q_G heat flux implies a decreasing cold content in the summer (Figure 8).

A comparison of surface energy balance of the Sutri Dhaka Glacier depicting similarities (and important differences) with other Himalayan glaciers is shown in Table 3. As previously observed for Himalayan glaciers (Yang et al., 2011; Zhang et al., 2013; Azam et al., 2014b; Singh et al., 2018; Patel et al., 2021), the current study also revealed that S_{net} is the predominant source of energy to the glacier surface and primarily determines the temporal variability of melting (Table 3). However, L_{net} is the largest energy sink that is substantially influenced by cloudy conditions. It is moderate during the summer, when L_{out} is nearly compensated by maximum L_{in} , due to the warm, humid, and cloudy environment, which decreases energy loss at the surface; and high during the winter, when L_{in} is at its lowest.

4.4 Surface mass balance

The modeled distributed surface mass balance values of the Sutri Dhaka Glacier revealed significant seasonal and interannual variability, with high positive values during the winter and stronger snow/ice mass loss during the summer (Table 4). The modeled glacier-wide annual balances were -1.09 ± 0.31 and -0.62 ± 0.19 m w.e. during 2015/16 and 2016/17, respectively (Figure 9 and Table 4). The values matched well with the observed values of -1.16 ± 0.33 and -0.67 ± 0.33 m w.e. during 2015/16 and 2016/17, respectively (Table 4). The ice loss

was higher in the lower ablation zone and decreased with an increase in altitude. The modeled mean annual mass balance for two balance years was -0.86 ± 0.21 m w.e. a^{-1} , which was similar to the mass balance reported by Sharma et al. (2020) based on the field results (-0.82 ± 0.17 m w.e. a^{-1} for 2013–2017). Our findings are also consistent with the study of Patel et al. (2021), who estimated an annual mass balance of -0.74 ± 0.1 m w.e. a^{-1} for the Sutri Dhaka Glacier during 2013–2019. However, our estimated mass balance is more negative than the Chhota Shigri Glacier that has a value of -0.46 ± 0.40 m w.e. a^{-1} for the period 2002–2019 (Mandal et al., 2020). The estimated geodetic mass balance for the Chandra basin is -0.68 ± 0.15 and -0.65 ± 0.43 m w.e. a^{-1} for the periods 1999–2011 and 2000–2012, respectively (Gardelle et al., 2013; Vijay and Braun, 2016), which is close to our estimate.

The modeled (observed) ELA was $5,368 \pm 10$ ($5,398 \pm 55$) m a.s.l. and $5,291 \pm 12$ ($5,295 \pm 69$) m a.s.l. during the year 2015/16 and 2016/17, respectively (Figure 9 and Table 4). The observed and model ELA of the Sutri Dhaka Glacier was higher than the observed ELA of Chhota Shigri Glacier (i.e., $5,047 \pm 104$ m a.s.l.) (Mandal et al., 2020).

4.5 Contrasting climatic variables as drivers for glacier mass balance

Among the climate variables, summer T_{air} was slightly higher (3.8°C) for 2015/16 than 2016/17 (3.3°C) (Table 5). Precipitation amount differed considerably between 2015/16 and 2016/17 at the Sutri Dhaka Glacier, with winter precipitation varying between 387 and 548 mm, respectively. It was similar in summer for both years (181 mm in 2015/16 and 162 mm in 2016/17) (Table 5). As a result, annual precipitation was substantially less (567 mm) during 2015/16 compared to 2016/17 (710 mm) (Table 5). Our study revealed that due to a substantially low snow accumulation the preceding winter, an early melt occurred (at a rate of ~ 0.009 m w.e. day^{-1}) during 2015/16 (from 5th March 2016), which was about 35 days in advance compared to 2016/17 (from 9th April 2017). This led to an enhanced melting of glacier ice in 2015/16, due to an early exposure of glacier ice. Therefore, two distinct annual mass balance results were observed for the two balance years

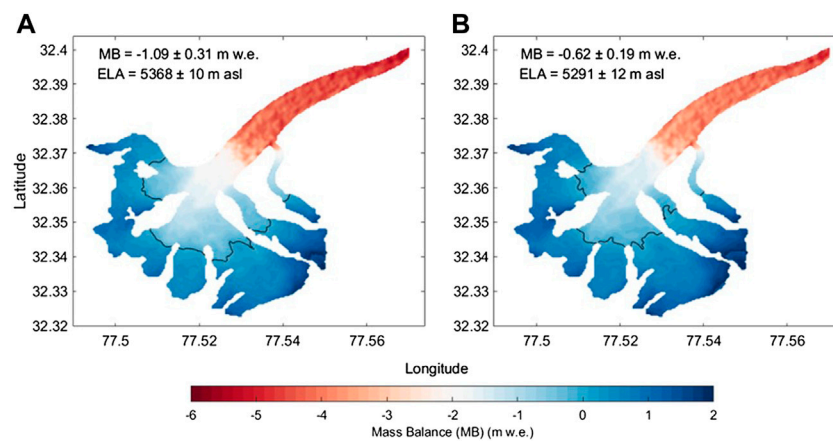


FIGURE 9

Spatial distribution of modeled annual mass balance at the Sutri Dhaka Glacier for the balance years (A) 2015/16 and (B) 2016/17. The black line indicates the equilibrium line altitude (ELA).

TABLE 5 Mean seasonal and annual meteorological variables and energy fluxes over the Sutri Dhaka Glacier, for study period from October 2015 to September 2017.

Variables	2015/16			2016/17			All observed period
	Winter	Summer	Annual	Winter	Summer	Annual	
T_{air} (°C)	-9.4	3.8	-4.6	-10.7	3.3	-4.4	-4.5
T_{surf} (°C)	-14.4	-2.1	-11.0	-17.6	-2.2	-9.6	-10.3
RH (%)	47	67	56	48	69	56	56
WS (m s^{-1})	3.8	3.4	3.6	3.6	3.3	3.5	3.6
Precipi (mm)	387	181	567	548	162	710	-
Press (hPa)	600	602	601	600	602	601	601
Cloud Cover	0.5	0.7	0.6	0.5	0.8	0.6	0.6
S_{in} (Wm^{-2})	217	294	248	192	288	233	240
S_{refl} (Wm^{-2})	116	92	112	141	106	121	116
Albedo	0.7	0.3	0.5	0.8	0.4	0.6	0.6
L_{in} (Wm^{-2})	196	260	223	202	264	227	225
L_{out} (Wm^{-2})	247	309	273	263	311	282	277
S_{net} (Wm^{-2})	101	202	136	51	181	112	124
L_{net} (Wm^{-2})	-51	-49	-50	-61	-47	-55	-52
H_{se} (Wm^{-2})	-6	22	6	-7	20	4	5
H_{la} (Wm^{-2})	-12	1	-6	-17	0	-10	-8
Q_{G} (Wm^{-2})	8	-8	1	6	-7	1	1
Q_{melt} (Wm^{-2})	13	181	79	9	170	77	78

(Table 4). The resulting spatially distributed annual mass balance for the period 2015/16 and 2016/17 are shown in Figure 9.

To explore the impact of seasonality and type of precipitation in controlling the annual mass balance of the Sutri Dhaka Glacier, we examined the precipitation rates and partition for

the balance years 2015/16 and 2016/17. The modeled daily mean precipitation rates were 13.19 and 17.91 mm w.e. d^{-1} during 2015/16 and 2016/17, respectively. During the winter, the mean daily rates of snowfall (rainfall) were 16.01 (0.00) and 23.76 (0.00) mm w.e. d^{-1} for 2015/16 and 2016/17, respectively. In

TABLE 6 Sensitivities of Sutri Dhaka Glacier mass balance to air temperature (T_{air}), precipitation (P), relative humidity (RH), incoming shortwave radiations (S_{in}), and wind speed (u).

Variables	Perturbation	Mass balance change (m w.e.)	Sensitivity
T_{air}	+1°C	-0.25 (29%)	-0.21 m w.e. a ⁻¹ °C ⁻¹
T_{air}	-1°C	0.15 (17%)	
P	+10%	0.21 (24%)	0.19 m w.e. a ⁻¹ (10%) ⁻¹
P	-10%	-0.17 (20%)	
RH	+10%	-0.10 (12%)	-0.10 m w.e. a ⁻¹ (10%) ⁻¹
RH	-10%	0.11 (13%)	
S_{in}	+50 Wm ⁻²	-0.09 (10%)	-0.09 m w.e. a ⁻¹ (50 Wm ⁻²) ⁻¹
S_{in}	-50 Wm ⁻²	0.1 (12%)	
u	+1 m s ⁻¹	-0.02 (2%)	-0.005 m w.e. a ⁻¹ (m s ⁻¹) ⁻¹
u	-1 m s ⁻¹	0.009 (1%)	

comparison, during the summer, the mean daily rates of snowfall (rainfall) were 3.31 (2.73) and 4.06 (2.26) mm w.e. d⁻¹ for 2015/16 and 2016/17, respectively. Therefore, the nearly 33% increase in winter snowfall, slightly enhanced summer snowfall and slightly reduced rainfall during 2016/17 led to reduced glacier melt compared to 2015/16.

5 Discussion

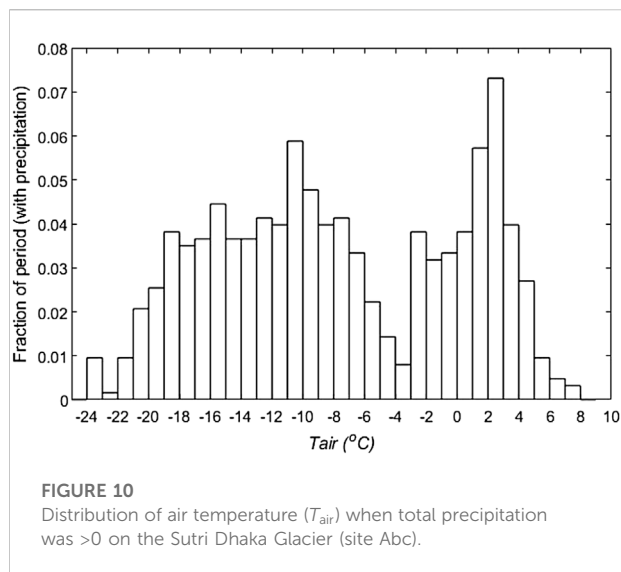
5.1 Sensitivity of glacier mass balance to climatic conditions

The climatic sensitivity of mass balance for the Sutri Dhaka Glacier was estimated using climatic variables and related simulations (Table 6). The model results suggest a decrease of mean annual mass balance of -0.25 m w.e. (29%) over an increase of 1°C in the T_{air} , whereas an increase of 0.15 m w.e. (17%) in the mean annual mass balance over a decrease in T_{air} by 1°C. With a 10% increase in precipitation, the mean annual mass balance was increased by 0.21 m w.e. (24%), whereas it decreased by -0.17 m w.e. (20%) with a decrease of precipitation by 10% for the Sutri Dhaka Glacier. Therefore, the mass balance sensitivity for T_{air} and precipitation change for the Sutri Dhaka Glacier was -0.21 m w.e. a⁻¹ °C⁻¹ and 0.19 m w.e. a⁻¹ (10%)⁻¹, respectively. With the increase in temperature, the melt seasons will be longer and thus the warming scenario will have increased mass balance sensitivity. Furthermore, the refreezing decreases as the temperature increases, which promotes further melting and as a result the glaciers can become more sensitive as the temperature keeps rising. However, if the temperature drops, there will be more refreezing conditions, and the glacier mass balance sensitivity will be reduced as compared to the rise in temperature. An increase in precipitation directly increases the snow accumulation, thus increasing the surface albedo, which

results in higher glacier mass balance sensitivity (Mölg et al., 2009). The amount of melt energy during the summer period, seasonal precipitation, and characteristics of surface topography may thus account for the difference in the mass balance sensitivity.

A comparison with other glaciers in the region indicated that the mass balance sensitivity to T_{air} for the Sutri Dhaka Glacier is significantly lower than that of the Chhota Shigri glacier (-0.52 m w.e. a⁻¹°C⁻¹) (Azam et al., 2014a) and is closer to that Stok glacier in Ladakh region (-0.32 m w.e. a⁻¹°C⁻¹) (Soheb et al., 2020). Similarly, mass balance sensitivity of precipitation was consistent with Stok Glacier (0.12 m w.e. a⁻¹ (10%)⁻¹) (Soheb et al., 2020). The mass balance sensitivity for relative humidity, S_{in} and wind speed change for the Sutri Dhaka Glacier was -0.10 m w.e. a⁻¹ (10%)⁻¹, -0.09 m w.e. a⁻¹ (50 Wm⁻²)⁻¹, and -0.005 m w.e. a⁻¹ (m s⁻¹)⁻¹, respectively. This is similar to Urumqi River Glacier No.1 in the Tien Shan, where a change in relative humidity by ±10%, reduced the glacier mass balance by 9% and increased by 8%, whereas a change in S_{in} by ±50 Wm⁻² decreased the glacier mass balance by 10% and increased by 8% (Che et al., 2019).

The temperature variability not only controls that of the melt but also influences the partitioning of the precipitation into snow or rain. The latter process has a potentially strong impact on the energy balance due to an associated albedo feedback. Following Cullen and Conway (2015), we investigated the role of the snow-to-rain partitioning on the mass balance of the Sutri Dhaka Glacier by considering the frequency distribution of daily mean T_{air} on the days with non-zero precipitation. The distribution of T_{air} during periods of precipitation resulted in a bimodal distribution (Figure 10). There was a broad peak in the range -21°C to -5°C, which suggests that 60% of the precipitation events occurred on winter days with temperatures less than -5°C. In contrast, the summer peak is associated with ISM (-3 to 5°C). Due to these differences, the snow-to-rain ratio is only weakly dependent on the temperature



on the Sutri Dhaka Glacier with a 4% decline in snowfall for a 1°C rise in T_{air} . Consequently, the T_{air} sensitivity of mass balance on the Sutri Dhaka Glacier is about ~ 6 times smaller than that on the Halji Glacier in the central Himalaya ($-1.43 \text{ m w.e. a}^{-1}\text{C}^{-1}$) (Arndt et al., 2021). Therefore, if all other factors remain the same, western Himalayan glaciers such as the Sutri Dhaka Glacier are likely to have a weaker mass balance response to temperature variability, and change than their central and eastern Himalayan counterparts (Fujita, 2008; Kumar et al., 2019). However, because our study consists of only two years of data, its representativeness for understanding future changes requires extended observations and additional analysis.

5.2 Implications and future perspectives

The current approach employing a well-constrained energy balance model demonstrates its ability to realistically simulate the distributed surface energy and mass balance of the Sutri Dhaka Glacier in the western Himalaya. Given that the model output corresponded well with the field measurements for two contrasting meteorological years, it supports the robustness of the model for its extended application for other Himalayan glaciers. Recent studies showed that most of the glaciers in the Hindu Kush Himalaya region are losing volume and mass due to increasing temperature caused by climate change (Immerzeel et al., 2010; Kraaijenbrink et al., 2017; Hock et al., 2019). Our study revealed that the glaciers in the Chandra basin of western Himalaya are highly sensitive to variations in precipitation and T_{air} , compared to other meteorological variables (Table 6). However, the sensitivity of Sutri Dhaka Glacier mass balance for precipitation partitioning (snow-to-

rain) to changes in T_{air} is low because the majority of precipitation occurs as snowfall during the cold winters. Several areas in the Hindu Kush Himalayan region have exhibited declining trends in snowfall in recent decades and future projections using multi-model ensembles also suggest a significant decrease in snowfall in several regions in the future in the Himalaya (Lutz et al., 2014; Sabin et al., 2020; Azam et al., 2021). Future projection studies also indicate that increasing temperature and decreasing solid precipitation will result in increased liquid precipitation, and extreme rainfall events may become more frequent and intense during the ablation seasons in the Hindu Kush Himalayan region (Lutz et al., 2014; Panday et al., 2015; Sanjay et al., 2017; Hock et al., 2019). An increase in liquid precipitation during the ablation season would result in increased total annual runoff that would enhance the glacier ice melt, favoring glacier mass loss and retreat (Bookhagen and Burbank, 2010; Lutz et al., 2014; Krishnan et al., 2019; Tawde et al., 2019; Azam et al., 2021). Although our study suggests that the Sutri Dhaka Glacier currently receives most of its precipitation during the cold winters, any future change in ISM and WD in a changing climate scenario can adversely impact the precipitation amount/phase and glacier mass balance in the region.

The present study is limited in extent, and therefore has some limitations. The differences in observed and modeled mass balance in the lower ablation area could be attributed to local factors such as the deposition of more dust at the beginning of the melt season, the presence of cryoconite holes, and debris cover. Due to these local factors, the lower ablation area may experience lower albedo and enhance the absorption of shortwave radiation, leading to higher melting than predicted. Observations of surface characteristics are required to impact the albedo parameterization of these processes in glacier models to minimize uncertainty in simulations (Collier et al., 2015; Soncini et al., 2017; Buri and Pellicciotti, 2018). The uncertainty of distributed meteorological variables is difficult to describe for glaciers due to local factors and micro-meteorological impacts (Shaw et al., 2021). Furthermore, other warm-air processes, such as the nonlinear effect of katabatic winds, impact of debris, and valley heating, may affect the lower ablation area of glaciers (Shea and Moore, 2010; Ayala et al., 2015; Shaw et al., 2021). Due to the variability of these effects, the melt rate is diverse and complex over the lower ablation area. Long-term datasets are required to examine the variability and implications of meteorological forcing during highly varying climatic conditions across different glaciers. Such long-term observations, integrated with climate model output, will be necessary for developing and validating glaciological and meteorological models for the Himalayan region. This would allow researchers to investigate the impact of ongoing and future climate variability on glaciers and hydrology.

6 Conclusion

We derived the distributed surface energy and mass balance of the Sutri Dhaka Glacier in the western Himalaya using a physically based model (COSIMA) in response to atmospheric forcing, and compared the results with glaciological mass balance observations during two contrasting meteorological years. First, we simulated surface energy and mass balance at the observed point location and calibrated it with the stakes-based glaciological mass balance data. The simulated surface albedo, incoming longwave radiation, and surface temperature using the model corresponded well with the observed values. Comparison of model output with the *in situ* observations suggests that the model performed well, and is therefore reliable for simulating distributed surface energy and mass balance. Seasonal variations in energy fluxes were dominated by changes in S_{net} and L_{net} fluxes, which significantly governed the mass balance of the Sutri Dhaka Glacier. The model-derived mean annual mass balances of -1.09 ± 0.31 and -0.62 ± 0.19 m w.e. for 2015/16 and 2016/17 are similar to the measured values of -1.16 ± 0.33 and -0.67 ± 0.33 m w.e., respectively. The sensitivity analysis shows that the mass balance of the Sutri Dhaka Glacier is affected by air temperature (-0.21 m w.e. $a^{-1} \text{ } ^\circ\text{C}^{-1}$) and precipitation (0.19 m w.e. a^{-1} (10%) $^{-1}$) changes. The present study suggests that the partitioning of precipitation into snow and rain is less sensitive to temperature changes for glacier mass balance because most precipitation falls as snow during the cold winters in the western Himalaya. Our study provides an opportunity for improved prediction of the surface mass balance of western Himalayan glaciers in a future climate change scenario.

Data availability statement

The raw data supporting the conclusions of this article will be made available by the authors, without undue reservation.

Author contributions

SNO, PS, and MT defined the objectives and designed the study. SNO, PS, BP, AS, and LKP collected the field data. SNO and BP performed the calculations. SNO, BP, MT, MR, AS, and AP interpreted the results. All authors contributed to the interpretation and discussion of the manuscript.

References

- Arndt, A., Scherer, D., and Schneider, C. (2021). Atmosphere driven mass-balance sensitivity of halji glacier, himalayas. *Atmosphere* 12, 426. doi:10.3390/atmos12040426
- Ayala, A., Pellicciotti, F., and Shea, J. M. (2015). Modeling 2m air temperatures over mountain glaciers: exploring the influence of katabatic

Funding

We thank the Ministry of Earth Sciences for financial support through the project “PACER—Cryosphere and Climate”.

Acknowledgments

We are thankful to the Director, National Centre for Polar and Ocean Research (NCPOR) for supporting the research at NCPOR. We acknowledge Argha Banerjee from the Indian Institute of Science Education and Research (IISER), Pune, for his critical suggestions and a careful review of this manuscript. The first author would like to thank Rahul Dey, Mohammad Nuruzzama and Vikram Goel for their valuable comments. We are grateful to ECMWF-ERA5 and SRTM teams for providing the data through their websites. We are also thankful to our field support team who were involved in our field trips. We thank scientific editor Nozomu Takeuchi and reviewers (Shin Sugiyama and Qiang Liu) for their helpful comments. This is NCPOR contribution no. J-28/2022-23..

Conflict of interest

The authors declare that the research was conducted in the absence of any commercial or financial relationships that could be construed as a potential conflict of interest.

Publisher's note

All claims expressed in this article are solely those of the authors and do not necessarily represent those of their affiliated organizations, or those of the publisher, the editors and the reviewers. Any product that may be evaluated in this article, or claim that may be made by its manufacturer, is not guaranteed or endorsed by the publisher.

Supplementary material

The Supplementary Material for this article can be found online at: <https://www.frontiersin.org/articles/10.3389/feart.2022.949735/full#supplementary-material>

cooling and external warming. *J. Geophys. Res. Atmos.* 120, 3139–3157. doi:10.1002/2015jd023137

Azam, M. F., Kargel, J. S., Shea, J. M., Nepal, S., Haritashya, U. K., Srivastava, S., et al. (2021). Glaciohydrology of the himalaya-karakoram. *Science* 373, eabf3668. doi:10.1126/science.abf3668

- Azam, M. F., Ramanathan, A., Wagnon, P., Vincent, C., Linda, A., Berthier, E., et al. (2016). Meteorological conditions, seasonal and annual mass balances of chhota shigri glacier, western himalaya, India. *Ann. Glaciol.* 57, 328–338. doi:10.3189/2016AoG71A570
- Azam, M. F., Wagnon, P., Ramanathan, A., Vinicent, C., Sharma, P., Arnaud, Y., et al. (2012). From balance to imbalance: a shift in the dynamic behaviour of chhota shigri glacier, western himalaya, India. *J. Glaciol.* 58, 315–324. doi:10.3189/2012JoG11J123
- Azam, M. F., Wagnon, P., Vincent, C., Ramanathan, A., Favier, V., Mandal, A., et al. (2014b). Processes governing the mass balance of chhota shigri glacier (Western Himalaya, India) assessed by point-scale surface energy balance measurements. *Cryosphere* 8, 2195–2217. doi:10.5194/tc-8-2195-2014
- Azam, M. F., Wagnon, P., Vincent, C., Ramanathan, A., Linda, A., Singh, V. B., et al. (2014a). Reconstruction of the annual mass balance of chhota shigri glacier, western Himalaya, India, since 1969. *Ann. Glaciol.* 55, 69–80. doi:10.3189/2014AoG66A104
- Azam, M. F., Wagnon, P., Vincent, C., Ramanathan, A. L., Kumar, N., Srivastava, S., et al. (2019). Snow and ice melt contributions in a highly glacierized catchment of chhota shigri glacier (India) over the last five decades. *J. Hydrology* 574, 760–773. doi:10.1016/j.jhydrol.2019.04.075
- Azam, M., Wagnon, P., Berthier, E., Vincent, C., Fujita, K., Js, K., et al. (2018). Review of the status and mass changes of himalayan-karakoram glaciers. *J. Glaciol.* 64, 61–74. doi:10.1017/jog.2017.86
- Bolch, T., Kulkarni, A., Kääb, A., Huggel, C., Paul, F., Cogley, J. G., et al. (2012). The state and fate of himalayan glaciers. *Science* 336, 310–314. doi:10.1126/science.1215828
- Bookhagen, B., and Burbank, D. W. (2006). Correction to “Topography, relief, and TRMM-derived rainfall variations along the Himalaya”. *Geophys. Res. Lett.* 33, L13402. doi:10.1029/2006gl026944
- Bookhagen, B., and Burbank, D. W. (2010). Toward a complete Himalayan hydrological budget: spatiotemporal distribution of snowmelt and rainfall and their impact on river discharge. *J. Geophys. Res.* 115, F03019. doi:10.1029/2009jf001426
- Brock, B. W., Willis, I. C., and Shaw, M. J. (2006). Measurement and parameterization of aerodynamic roughness length variations at haut glacier d’Arolla, Switzerland. *J. Glaciol.* 52, 281–297. doi:10.3189/172756506781828746
- Brun, F., Berthier, E., Wagnon, P., Kääb, A., and Treichler, D. (2017). A spatially resolved estimate of high mountain asia glacier mass balances from 2000 to 2016. *Nat. Geosci.* 10, 668–+, 673. doi:10.1038/ngeo2999
- Buri, P., and Pellicciotti, F. (2018). Aspect controls the survival of ice cliffs on debris-covered glaciers. *Proc. Natl. Acad. Sci. U. S. A.* 115, 4369–4374. doi:10.1073/pnas.1713892115
- Che, Y. J., Zhang, M. J., Li, Z. Q., Wei, Y. Q., Nan, Z. T., Li, H. L., et al. (2019). Energy balance model of mass balance and its sensitivity to meteorological variability on urumqi river glacier No.1 in the chinese tien shan. *Sci. Rep.* 9, 13958. doi:10.1038/s41598-019-50398-4
- Cogley, J. G., Hock, R., Rasmussen, L. A., Arendt, A. A., Bauder, A., Braithwaite, R. J., et al. (2011). Glossary of glacier mass balance and related terms.” in *IHP IHP-VII technical documents in hydrology No. 86, IACS contribution No. 2*. Paris/Paris, France: UNESCO/UNESCO-IHP.
- Collier, E., Maussion, F., Nicholson, L. I., Mölg, T., Immerzeel, W. W., Bush, A. B. G., et al. (2015). Impact of debris cover on glacier ablation and atmosphere-glacier feedbacks in the karakoram. *Cryosphere* 9, 1617–1632. doi:10.5194/tc-9-1617-2015
- Cullen, N. J., and Conway, J. P. (2015). A 22 month record of surface meteorology and energy balance from the ablation zone of brewster glacier, new zealand. *J. Glaciol.* 61, 931–946. doi:10.3189/2015JoG15J004
- Cullen, N. J., Mölg, T., Kaser, G., Steffen, K., and Hardy, D. R. (2007). Energy-balance model validation on the top of kilimanjaro, tanzania, using eddy covariance data. *Ann. Glaciol.* 46, 227–233. doi:10.3189/172756407782871224
- De Woul, M., and Hock, R. (2005). “Static mass-balance sensitivity of Arctic glaciers and ice caps using a degree-day approach.”. Editors J. Dowdeswell and I. C. Willis, Vol. 42, 2005217–2005224. *Ann. Glaciol.*
- Dimri, A. P., Niyogi, D., Barros, A. P., Ridley, J., Mohanty, U. C., Yasunari, T., et al. (2015). Western disturbances: a review. *Rev. Geophys.* 53, 225–246. doi:10.1002/2014rg000460
- Dyrgerov, M. B., and Meier, M. F. (2005). ColoradoBoulder.” in *Glaciers and the changing earth system: A 2004 snapshot*, 58: Institute of Arctic and Alpine Research, University of Colorado, Occasional Paper, 117.
- Farinotti, D., Immerzeel, W. W., De Kok, R. J., Quincey, D. J., and Dehecq, A. (2020). Manifestations and mechanisms of the Karakoram glacier anomaly. *Nat. Geosci.* 13, 8. doi:10.1038/s41561-019-0513-5
- Fujita, K. (2008). Effect of precipitation seasonality on climatic sensitivity of glacier mass balance. *Earth Planet. Sci. Lett.* 276, 14–19. doi:10.1016/j.epsl.2008.08.028
- Gardelle, J., Berthier, E., Arnaud, Y., and Kääb, A. (2013). Corrigendum to “Region-wide glacier mass balances over the Pamir-karakoram-himalaya during 1999–2011” published in the *Cryosphere*, 7, 1263–1286, 2013. *Cryosphere* 7, 1885–1886. doi:10.5194/tc-7-1885-2013
- Giesen, R. H., Andreassen, L. M., Van Den Broeke, M. R., and Oerlemans, J. (2009). Comparison of the meteorology and surface energy balance at storbreen and middalsbreen, two glaciers in southern Norway. *Cryosphere* 3, 57–74. doi:10.5194/tc-3-57-2009
- Gromke, C., Manes, C., Walter, B., Lehning, M., and Guala, M. (2011). Aerodynamic roughness length of fresh snow. *Bound. Layer. Meteorol.* 141, 21–34. doi:10.1007/s10546-011-9623-3
- Hock, R., and Holmgren, B. (2005). A distributed surface energy-balance model for complex topography and its application to Storglaciaren, Sweden. *J. Glaciol.* 51, 25–36. doi:10.3189/172756505781829566
- Hock, R. (2003). Temperature index melt modelling in mountain areas. *J. Hydrology* 282, 104–115. doi:10.1016/s0022-1694(03)00257-9
- Hock, R., Rasul, G., Adler, C., Cáceres, B., Gruber, S., Hirabayashi, Y., et al. (2019). “IPCC ocean and cryosphere in a changing climate, Chap 2,” in *High mountain areas*.
- Huintjes, E., Sauter, T., Schroter, B., Maussion, F., Yang, W., Kropacek, J., et al. (2015). Evaluation of a coupled snow and energy balance model for zhadang glacier, tibetan plateau, using glaciological measurements and time-lapse photography. *Arct. Antarct. Alp. Res.* 47, 573–590. doi:10.1657/aaar0014-073
- Immerzeel, W. W., Van Beek, L. P. H., and Bierkens, M. F. P. (2010). Climate change will affect the asian water towers. *Science* 328, 1382–1385. doi:10.1126/science.1183188
- Jean-Philippe, B., Michael, H., and Petrie, C. A. (2021). Synoptic processes of winter precipitation in the upper indus basin. *Weather Clim. Dynam.* 2, 1187–1207. doi:10.5194/wcd-2-1187-2021
- Kääb, A., Berthier, E., Nuth, C., Gardelle, J., and Arnaud, Y. (2012). Contrasting patterns of early twenty-first-century glacier mass change in the himalayas. *Nature* 488, 495–498. doi:10.1038/nature11324
- Kayastha, R. B., Ohata, T., and Ageta, Y. (1999). Application of a mass-balance model to a himalayan glacier. *J. Glaciol.* 45, 559–567. doi:10.3189/s002214300000143x
- Kenzebeaev, R., Barandun, M., Kronenberg, M., Chen, Y. N., Usualiev, R., Hoelzle, M., et al. (2017). Mass balance observations and reconstruction for batysh sook glacier, tien shan, from 2004 to 2016. *Cold Regions Sci. Technol.* 135, 76–89. doi:10.1016/j.coldregions.2016.12.007
- Klok, E. J., and Oerlemans, J. (2002). Model study of the spatial distribution of the energy and mass balance of morteratschgletscher, Switzerland. *J. Glaciol.* 48, 505–518. doi:10.3189/172756502781831133
- Kraaijenbrink, P. D. A., Bierkens, M. F. P., Lutz, A. F., and Immerzeel, W. W. (2017). Impact of a global temperature rise of 1.5 degrees Celsius on Asia’s glaciers. *Nature* 549, 257–+, 260. doi:10.1038/nature23878
- Krishnan, R., Shrestha, A. B., Ren, G., Rajbhandari, R., Saeed, S., Sanjay, S., et al. (2019). “Unravelling climate change in the hindu kush himalaya: rapid warming in the mountains and increasing extremes,” in *The Hindu Kush Himalaya assessment—mountains, climate change, sustainability and people*. Editors P. Wester, A. Mishra, A. Mukherji, and A. B. Shrestha (Cham: Springer), 57–97.
- Kulkarni, A. V., Bahuguna, I. M., Rathore, B. P., Singh, S. K., Randhawa, S. S., Sood, R. K., et al. (2007). Glacial retreat in Himalaya using Indian Remote Sensing satellite data. *Curr. Sci.* 92, 69–74.
- Kumar, A., Verma, A., Gokhale, A. A., Bhambri, R., Misra, A., Sundriyal, S., et al. (2018). Hydrometeorological assessments and suspended sediment delivery from a central Himalayan glacier in the upper Ganga basin. *Int. J. Sediment Res.* 33, 493–509. doi:10.1016/j.ijsrc.2018.03.004
- Kumar, L., Skidmore, A. K., and Knowles, E. (1997). Modelling topographic variation in solar radiation in a GIS environment. *Int. J. Geogr. Inf. Sci.* 11, 475–497. doi:10.1080/136588197242266
- Kumar, P., Saharwardi, M. S., Banerjee, A., Azam, M. F. A., Dubey, A. K., Murtugudde, R., et al. (2019). Snowfall variability dictates glacier mass balance variability in himalaya-karakoram. *Sci. Rep.* 9, 18192. doi:10.1038/s41598-019-54553-9
- Li, S. H., Yao, T. D., Yu, W. S., Yang, W., and Zhu, M. L. (2019). Energy and mass balance characteristics of the guliya ice cap in the west kunlun mountains, tibetan plateau. *Cold Regions Sci. Technol.* 159, 71–85. doi:10.1016/j.coldregions.2018.12.001

- Lutz, A. F., Immerzeel, W. W., Shrestha, A. B., and Bierkens, M. F. P. (2014). Consistent increase in high asia's runoff due to increasing glacier melt and precipitation. *Nat. Clim. Chang.* 4, 587–592. doi:10.1038/nclimate2237
- Machguth, H., Purves, R. S., Oerlemans, J., Hoelzle, M., and Paul, F. (2008). Exploring uncertainty in glacier mass balance modelling with monte carlo simulation. *Cryosphere* 2, 191–204. doi:10.5194/tc-2-191-2008
- Mandal, A., Ramanathan, A., Azam, M. F., Angchuk, T., Soheb, M., Kumar, N., et al. (2020). Understanding the interrelationships among mass balance, meteorology, discharge and surface velocity on chhota shigri glacier over 2002–2019 using *in situ* measurements. *J. Glaciol.* 66, 727–741. doi:10.1017/jog.2020.42
- Mölg, T., Cullen, N. J., Hardy, D. R., Winkler, M., and Kaser, G. (2009). Quantifying climate change in the tropical midtroposphere over east africa from glacier shrinkage on kilimanjaro. *J. Clim.* 22, 4162–4181. doi:10.1175/2009jcli2954.1
- Mölg, T., and Scherer, D. (2012). Retrieving important mass-balance model parameters from AWS measurements and high-resolution mesoscale atmospheric modeling. *J. Glaciol.* 58, 625–628. doi:10.3189/2012JG11J258
- Oerlemans, J. (2000). Analysis of a 3 year meteorological record from the ablation zone of morteratschgletscher, switzerland: energy and mass balance. *J. Glaciol.* 46, 571–579. doi:10.3189/172756500781832657
- Oerlemans, J. (2001). *Glaciers and climate change*. Lisse: Swets & Zeitlinger, 148.
- Oerlemans, J., and Knap, W. H. (1998). A 1 year record of global radiation and albedo in the ablation zone of morteratschgletscher, switzerland. *J. Glaciol.* 44, 231–238. doi:10.3189/s0022143000002574
- Oerlemans, J., and Reichert, B. K. (2000). Relating glacier mass balance to meteorological data by using a seasonal sensitivity characteristic. *J. Glaciol.* 46, 1–6. doi:10.3189/172756500781832629
- Østrem, G., and Brugman, M. (1991). Glacier mass-balance measurements.” in *A manual for field and office work. (NHRI Science Report 4*. Environment Canada/Saskatoon, Sask: National Hydrology Research Institute.
- Panday, P. K., Thibeault, J., and Frey, K. E. (2015). Changing temperature and precipitation extremes in the hindu kush-himalayan region: an analysis of CMIP3 and CMIP5 simulations and projections. *Int. J. Climatol.* 35, 3058–3077. doi:10.1002/joc.4192
- Patel, A., Goswami, A., Dharpure, J. K., Thamban, M., Sharma, P., Kulkarni, A. V., et al. (2021). Estimation of mass and energy balance of glaciers using a distributed energy balance model over the Chandra river basin (Western Himalaya). *Hydrol. Process.* 35, doi:10.1002/hyp.14058
- Pellicciotti, F., Carenzo, M., Helbing, J., Rimkus, S., and Burlando, P. (2009). On the role of subsurface heat conduction in glacier energy-balance modelling. *Ann. Glaciol.* 50, 16–24. doi:10.3189/172756409787769555
- Pratap, B., Dobhal, D. P., Bhambri, R., Mehta, M., and Tewari, V. C. (2016). Four decades of glacier mass balance observations in the Indian Himalaya. *Reg. Environ. Change* 16, 643–658. doi:10.1007/s10113-015-0791-4
- Pratap, B., Sharma, P., Patel, L. K., Singh, A. T., Gaddam, V. K., Oulkar, S., et al. (2019). Reconciling high glacier surface melting in summer with air temperature in the semi-arid zone of western Himalaya. *Water* 11, 1561. doi:10.3390/w11081561
- Pritchard, H. D. (2019). Asia's shrinking glaciers protect large populations from drought stress. *Nature* 569, 649–, 654. doi:10.1038/s41586-019-1240-1
- Sabin, T. P., Krishnan, R., Vellore, R., Priya, P., Bargaonkar, H. P., Singh, B. B., et al. (2020). “Climate change over the himalayas,” in *Assessment of climate change over the Indian region*. Editors R. Krishnan, J. Sanjay, C. Gnanaseelan, M. Mujumdar, A. Kulkarni, and S. Chakraborty (Springer, Singapore). doi:10.1007/978-981-15-4327-2_11
- Sangewar, C. V., and Shukla, S. P. (2009). *Inventory of the Himalayan glaciers: A contribution to the international hydrological programme*, 34. Spec. Publ. No. Geological Survey of India.
- Sanjay, J., Krishnan, R., Shrestha, A. B., Rajbhandari, R., and Ren, G. Y. (2017). Downscaled climate change projections for the hindu kush himalayan region using CORDEX south asia regional climate models. *Adv. Clim. Change Res.* 8, 185–198. doi:10.1016/j.accre.2017.08.003
- Sharma, P., Patel, L. K., Ravindra, R., Singh, A., Mahalinganathan, K., Thamban, M., et al. (2016). Role of debris cover to control specific ablation of adjoining batal and sutri dhaka glaciers in chandra basin (Himachal Pradesh) during peak ablation season. *J. Earth Syst. Sci.* 125, 459–473. doi:10.1007/s12040-016-0681-2
- Sharma, P., Patel, L. K., Singh, A. T., Meloth, T., and Ravindra, R. (2020). “Glacier response to climate in arctic and himalaya during last seventeen years: a case study of svalbard, arctic and chandra basin, himalaya,” in *Climate change and the white world*. Editors P. S. Goel, R. Ravindra, and S. Chattopadhyay (Springer), 139–156.
- Shaw, T. E., Yang, W., Ayala, A., Bravo, C., Zhao, C. X., Pellicciotti, F., et al. (2021). Distributed summer air temperatures across mountain glaciers in the south-east Tibetan plateau: temperature sensitivity and comparison with existing glacier datasets. *Cryosphere* 15, 595–614. doi:10.5194/tc-15-595-2021
- Shea, J. M., and Moore, R. D. (2010). Prediction of spatially distributed regional-scale fields of air temperature and vapor pressure over mountain glaciers. *J. Geophys. Res.* 115, D23107. doi:10.1029/2010jd014351
- Shean, D. E., Bhushan, S., Montesano, P., Rounce, D. R., Arendt, A., Osmanoglu, B., et al. (2020). A systematic, regional assessment of high mountain Asia glacier mass balance. *Front. Earth Sci. (Lausanne)*. 7. doi:10.3389/feart.2019.00363
- Shekhar, M. S., Chand, H., Kumar, S., Srinivasan, K., and Ganju, A. (2010). Climate-change studies in the Western Himalaya. *Ann. Glaciol.* 51, 105–112. doi:10.3189/172756410791386508
- Singh, A. T., Rahaman, W., Sharma, P., Laluraj, C. M., Patel, L. K., Pratap, B., et al. (2019). Moisture sources for precipitation and hydrograph components of the Sutri Dhaka glacier basin, western himalayas. *Water* 11, 2242. doi:10.3390/w11112242
- Singh, N., Singhal, M., Chhikara, S., Karakoti, I., Chauhan, P., Dobhal, D. P., et al. (2018). Radiation and energy balance dynamics over a rapidly receding glacier in the central Himalaya. *Int. J. Climatol.* 21, 400–420. doi:10.1002/joc.6218
- Soheb, M., Ramanathan, A., Angchuk, T., Mandal, A., Kumar, N., Lotus, S., et al. (2020). Mass-balance observation, reconstruction and sensitivity of Stok glacier, Ladakh region, India, between 1978 and 2019. *J. Glaciol.* 66, 627–642. doi:10.1017/jog.2020.34
- Soncini, A., Bocchiola, D., Azzone, R. S., and Diolaiuti, G. (2017). A methodology for monitoring and modeling of high altitude Alpine catchments. *Prog. Phys. Geogr. Earth Environ.* 41, 393–420. doi:10.1177/0309133317710832
- Sun, W. J., Qin, X., Wang, Y. T., Chen, J. Z., Du, W. T., Zhang, T., et al. (2018). The response of surface mass and energy balance of a continental glacier to climate variability, western qilian mountains, china. *Clim. Dyn.* 50, 3557–3570. doi:10.1007/s00382-017-3823-6
- Sunako, S., Fujita, K., Sakai, A., and Kayastha, R. B. (2019). Mass balance of trambau glacier, rolwaling region, nepal Himalaya: *in-situ* observations, long-term reconstruction and mass-balance sensitivity. *J. Glaciol.* 65, 605–616. doi:10.1017/jog.2019.37
- Tachikawa, T. (2011). *Characteristics of ASTER GDEM version 2 international geoscience and remote sensing symposium (IGARSS)*.
- Tawde, S. A., Kulkarni, A. V., and Bala, G. (2019). An assessment of climate change impacts on glacier mass balance and geometry in the chandra Basin, western himalaya for the 21st century. *Environ. Res. Commun.* 1, 041003. doi:10.1088/2515-7620/ab1d6d
- Thibert, E., Blanc, R., Vincent, C., and Eckert, N. (2008). Glaciological and volumetric mass-balance measurements: error analysis over 51 years for glacier de sarennes, french alps. *J. Glaciol.* 54, 522–532. doi:10.3189/002214308785837093
- Van Den Broeke, M., Reijmer, C., Van As, D., and Boot, W. (2006). Daily cycle of the surface energy balance in antarctica and the influence of clouds. *Int. J. Climatol.* 26, 1587–1605. doi:10.1002/joc.1323
- Van Der Veen, C. J. (2002). Polar ice sheets and global sea level: How well can we predict the future? *Glob. Planet. Change* 32, 165–194. doi:10.1016/s0921-8181(01)00140-0
- Vijay, S., and Braun, M. (2016). *Elevation Change Rates of Glaciers in the Lahaul-Spiti (Western Himalaya, India) during 2000-2012 and 2012-2013*, 8. doi:10.3390/rs8121038Remote Sens.
- Wagnon, P., Linda, A., Arnaud, Y., Kumar, R., Sharma, P., Vincent, C., et al. (2007). Four years of mass balance on chhota Shigri Glacier, Himachal Pradesh, India, a new benchmark glacier in the Western Himalaya. *J. Glaciol.* 53, 603–611. doi:10.3189/002214307784409306
- Wagnon, P., Vincent, C., Arnaud, Y., Berthier, E., Vuillermoz, E., Gruber, S., et al. (2013). Seasonal and annual mass balances of Mera and Pokalde glaciers (Nepal Himalaya) since 2007. *Cryosphere* 7, 1769–1786. doi:10.5194/tc-7-1769-2013
- WGMS (2019). *Fluctuations of glaciers database*. Zurich, Switzerland: World Glacier Monitoring Service. doi:10.5904/wgms-fog-2019-12
- Wu, X. J., He, J. Q., Jiang, X., and Wang, N. L. (2016). Analysis of surface energy and mass balance in the accumulation zone of Qiyi glacier, tibetan plateau in an ablation season. *Environ. Earth Sci.* 75, 785. doi:10.1007/s12665-016-5591-8
- Yang, W., Guo, X. F., Yao, T. D., Yang, K., Zhao, L., Li, S. H., et al. (2011). Summertime surface energy budget and ablation modeling in the ablation zone of a maritime tibetan glacier. *J. Geophys. Res.* 116, D14116. doi:10.1029/2010jd015183
- Yang, W., Yao, T. D., Guo, X. F., Zhu, M. L., Li, S. H., Kattel, D. B., et al. (2013). Mass balance of a maritime glacier on the southeast tibetan plateau and its climatic sensitivity. *J. Geophys. Res. Atmos.* 118, 9579–9594. doi:10.1002/jgrd.50760
- Zhang, G. S., Kang, S. C., Fujita, K., Huintjes, E., Xu, J. Q., Yamazaki, T., et al. (2013). Energy and mass balance of zhadang glacier surface, central tibetan plateau. *J. Glaciol.* 59, 137–148. doi:10.3189/2013JG12J152
- Zhu, M. L., Yao, T. D., Yang, W., Xu, B. Q., Wu, G. J., Wang, X. J., et al. (2018). Erratum to: differences in mass balance behavior for three glaciers from different climatic regions on the tibetan plateau. *Clim. Dyn.* 51, 769. doi:10.1007/s00382-017-3915-3